ELSEVIER

Detection of phosphorus oxyanions in synthetic geothermal water using ion chromatography–mass spectrometry techniques

Michelle M. Ivey, Krishna L. Foster*

Department of Chemistry and Biochemistry, California State University, 5151 State University Drive, Los Angeles, CA 90032-8282, USA

Abstract

Recent developments in microbiology suggest that reduced inorganic phosphorus oxyanions, including hypophosphite and phosphite, may be present in nature. These studies have inspired the development of specific and sensitive methods that detect phosphorus oxyanions in natural water. This paper will discuss a new technique that couples suppressed conductivity ion chromatography (Dionex AS17 analytical column and potassium hydroxide eluent) with electrospray mass spectrometry (IC/MS) with limits of detection nearly 200 times lower than those reported using suppressed conductivity detection. The technique was optimized for the detection of hypophosphite, phosphite, and phosphate in a synthetic geothermal water matrix. Samples were pre-treated with silver and sulfonic acid cartridges, and injection loop sizes as large as 800 μl were employed to enhance instrument sensitivity. All peaks were clearly resolved, and calibrations were linear with estimated 3σ limits of detection of 0.011, 0.0020, and 0.029 μM for hypophosphite, phosphite, and phosphate, respectively.
© 2005 Elsevier B.V. All rights reserved.

Keywords: Water analysis; Geochemistry; Phosphorus compounds; Hypophosphite; Phosphite; Phosphate

1. Introduction

Recent studies show microorganisms contain enzymes that metabolize reduced trivalent (III) phosphite and univalent (I) hypophosphite [1], suggesting that microorganisms can utilize phosphorus oyxanions in oxidation states other than pentavalent (V) phosphate, the most common form of bioavailable phosphorus. Moreover, highly reduced forms of phosphorus, namely phophine (III) have been detected in nature in reducing environments such as sewage [2,3], marine sediments [4], and in industrial [5] and agricultural [6] processes. In natural environments, phosphate is the only thermodynamically stable phosphorus oxyanion [7], and consequently the most abundant with measured concentrations ranging from 0.3 to 30 μM, in pristine environments [8]. Non-equilibrium states persist throughout nature, and consequently, hypophosphite and phosphite may be present at concentrations less than the micromolar concentrations of phosphate. The implications of measuring reduced phosphorus oxyanions in nature would be profound. These mea-

surements may help elucidate the mechanism of phosphine gas formation, and inspire the scientific community to reevaluate the cycling of phosphorus in biological systems. The first step towards measuring reduced phosphorus oxyanions is to develop new methods to detect sub-micromolar concentrations of these oxyanions in matrices representative of natural waters.

Geothermal waters are likely sites for the existence of naturally occurring reduced phosphorus oxyanions. Present in hot springs and oceanic vents, these waters are influenced by the reducing environment below the Earth's surface. Anions in this matrix include fluoride, chloride, bromide, nitrate, hydrogen carbonate, and sulfate. Methods for the detection of reduced phosphorus oxyanions include ion chromatography [9–16], ^{31}P NMR with D_2O locking [1], spectrophotometric determination in a flow injection system [17], and gas chromatography coupled with mass spectrometry [18]. Sample preparation for the ^{31}P NMR and flow injection techniques includes non-discriminatory oxidation processes that do not distinguish hypophosphite from phosphite. Ion chromatography is the most specific of the listed techniques. In the McDowell et al. study, hypophosphite, phosphite and phosphate were detected in a synthetic geothermal water matrix with reported 3σ limits of detection of 0.83, 0.39, and 0.35 μM, respectively, using ion chromatography with sup-

---

pressed conductivity detection [14]. These experiments were performed after diluting full strength synthetic geothermal water by a factor of four. Further improvement of the limits of detection could not be achieved with higher samples volumes and concentrations, because this was hindered by the inability to resolve the fluoride/hypophosphite, and phosphite/hydrogen carbonate peak pairs. Suppressed conductivity detection is a non-specific technique that detects anything that affects the resistivity of the solution through the conductivity cell. If background ions were removed from the matrix, or if ion chromatography were coupled with a detector that responds only to a specific characteristic of the analyte, then larger volumes and concentrations of sample could be delivered to the column, and consequently, limits of detection could be lowered.

Ion chromatography coupled with detectors with higher specificity, such as mass spectrometers or inductively coupled plasma (ICP) elemental detectors [9,11,16], provides the specificity necessary to improve the limits of detection for phosphorous oxyanions in complex matrices. Inductively coupled plasma detectors have been used to measure hypophosphite, phosphite and phosphate as ^{31}P in complex matrices with limits of detection near $10\,\mu g\,l^{-1}$. While ICP techniques are noted for their specificity in identification of elemental phosphourus, the sensitivity of these techniques is limited by the high ionization potential of elemental phosphorus [19]. Other specific detectors such as electrospray mass spectrometry coupled with ion chromatography have the potential to lower the limits of detection even further. This paper introduces a two-dimensional analytical technique that couples the resolution capabilities of ion chromatography with the specificity of electrospray mass spectrometry. The contributions of matrix simplification prior to analysis and variations in the concentrations and volumes of injected sample to the optimization of this technique will be discussed.

2. Methods

2.1. Standards

A 1 mM stock solution of three phosphorus oxyanions was prepared from the following individual stock solutions. Phosphate was used directly from a commercial potassium dihydrogen phosphate (KH_2PO_4) standard containing 1000 ppm of phosphate (LabChem Inc.). Hypophosphite and phosphite solutions were prepared by dissolving sodium hypophosphite monohydrate ($NaH_2PO_2 \cdot H_2O$, Sigma) and sodium phosphite-5-hydrate ($Na_2(PHO_3) \cdot 5H_2O$, Riedel-de Haën) in $18.2\,M\Omega\,cm$ Nanopure (Barnstead) water.

All studies were performed with equimolar concentrations of the three phosphorus oxyanions in synthetic geothermal water prepared from sodium salts. The phosphorus oxyanion concentrations varied from 0 to $10\,\mu M$, and the anion concentrations were determined from literature values for Hot Creek, a geothermal system near Mammoth Lakes, CA [20]. The anion concentrations were 8.1 mM hydrogen carbonate, 5.5 mM chloride, 0.91 mM sulfate, 0.81 mM bromide, 0.43 mM fluoride and 0.01 mM nitrate. Synthetic geothermal water stock solu-

tion was prepared from sodium hydrogen carbonate (Certified ACS grade, Fisher Scientific), sodium chloride (Certified ACS grade, Fisher Scientific), anhydrous sodium sulfate (Certified ACS grade, Fisher Scientific), sodium bromide (Certified ACS grade, Fisher Scientific), sodium fluoride solution (standardized 0.100 M, Fisher Scientific) and sodium nitrate solution (1000 ppm, 98%, SPEX CertiPrep). All solutions prepared from salts were filtered with $0.2\,\mu m$ cellulose acetate filters, stored in HDPE bottles at $4\,°C$, and used within 30 days of preparation.

2.2. Sample preparation

The results of simplifying the geothermal matrix by removing superfluous anions including chloride, bromide and hydrogen carbonate were examined in this study. Samples were filtered through two OnGuard II cartridges (silver, Dionex p/n 057089 and sulfonic acid, Dionex p/n 057085) connected in series [21]. The first cartridge contained silver ions, which removed chloride and bromide by the precipitation of insoluble silver chloride and silver bromide salts. The second cartridge contained a styrene-based, strong resin in the H^+ form, which has a strong affinity for multivalent cations, and would also trap any silver ion breakthrough from the first cartridge. The second cartridge also converted carbonate to carbonic acid, which was then removed by sparging with nitrogen (UHP, Gilmore Liquid-Air) for 5 min to accelerate the removal of carbon dioxide gas from the system [21].

2.3. Ion chromatography system with conductivity detector

Two Dionex DX 600 suppressed conductivity ion chromatography (IC) systems were employed in this study. The first utilized a GS50 gradient pump, an AS50 autosampler, and a CD25 conductivity detector. The second system was equipped with a LC20 chromatography compartment, an IP25 isocratic pump and a CD20 conductivity detector. Both systems employed hydrophilic quaternary ammonium functionalized 4 mm analytical columns (Dionex IonPac AS17), preceded by guard columns (Dionex IonPac AG17) for anion separation; EG40 electrolytic eluent generators; and ASRS Ultra II suppressors. All samples were refrigerated prior to injection.

Potassium hydroxide eluent was generated electrolytically. Degassed $18.2\,M\Omega\,cm$ Nanopure water was stored in a 4 l plastic bottle under 40 kPa UHP helium. An ATC-3 trap column was used to strip trace anion contaminants from the water before the water was pumped at $1.5\,ml\,min^{-1}$ into a Dionex EG40 eluent generator where the potassium hydroxide eluent was generated electrolytically. The gradient was as follows: 0.5 mM from 0 to 5 min; 0.5–9 mM from 5 to 13 min; 9.0 mM between 13 and 16 min; 9.0–35.0 from 16 to 18 min, and 35 mM from 18 to 20 min. This gradient was adjusted throughout the study to compensate for retention time shifts attributed to column aging [22].

After separation, the eluent stream was directed through a suppressor (Dionex ASRS Ultra II, current 300 mA), which converted the hydroxide eluent to water, resulting in anions in neutral pH water, which could then be monitored via a conductivity detector. The suppressor was regenerated with an external
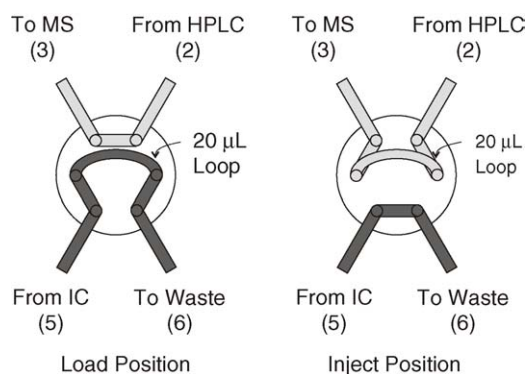
Fig. 1. Schematic of the six-port pulsed-fraction-injection valve illustrating the 20 μl fraction-collector loop "load" and "inject" positions.

18.2 MΩ cm water source that was pumped through the suppressor at a rate of ~2 ml min^{-1} with a peristaltic pump (The Pump Works Inc. 1000). Because an external water source was used rather than using the effluent to regenerate the suppressor, the eluent could be directed into another detector, such as a mass spectrometer.

2.4. Pulsed fraction injections at the IC/ESI-MS interface

The pH neutral effluent was directed through a ThermoFinnigan LCQ Deca ion-trap mass spectrometer attached in series with the conductivity detector. To interface the IC with the electrospray ionization mass spectrometer (ESI-MS), it was necessary to remove the backpressure coil normally located after the conductivity detector. The backpressure coil was replaced with 36 in. of 0.010 in. I.D. PEEK tubing used to deliver the eluent to a six-port injection valve (VICI Valco C3-2006EH). This injector was used to inject fractions of the IC effluent stream into the mass spectrometer. A LabView program was used, in conjunction with a relay box (National Instruments, ER-16) to control the valve actuator. A schematic of the "load" and "inject" positions of the pulsed fraction injector is presented in Fig. 1. The valve was equipped with a 20 μl fraction collector loop (Vici, CSL 20) across ports 1 and 4. When the valve was in the load position, the chromatographic effluent entered the valve at port 5, filling the loop before flowing out to waste (port 6). During this time, water pumped with an HPLC pump (Surveyor, ThermoFinnigan) entered the valve at 500 μl min^{-1} through port 2, and was directed to the mass spectrometer inlet (port 3). When the valve was switched to the inject position, the IC effluent was diverted directly to waste (port 6) while the water from the HPLC pump (port 2) was used to direct the IC fraction contained in the loop into the mass spectrometer (port 3). The valve was toggled between positions every second.

2.5. Electrospray mass spectrometry detector

The mass spectrometer was configured with electrospray ionization operated with 8 kV on the needle, and the heated capillary tubing was held at 350 °C. Although volatile organic solvents such as methanol and acetonitrile are typically com-

bined with water for electrospray ionization, 100% water was used in the current study. To accommodate for low volatility of the solvent, the electrospray nozzle was fully retracted, and the sheath gas was maintained at 80 (arbitrary units). Selection criteria for these parameters are discussed further in section 3.1 of this article. Mass spectra were collected from $m/z = 50$ to 100, and signal to noise was improved by averaging 10 spectra. The mass-to-charge ratio of 50 is the lowest that can be detected by the LCQ Deca mass spectrometer. Consequently, only singly charged phosphorus oxyanions were detected in this study, although about 50% of phosphite and phosphate are doubly charged at near neutral pH [7,14]. Hypophosphite ($H_2PO_2^-$), phosphite ($H_2PO_3^-$), and phosphate ($H_2PO_4^-$) were detected at $m/z = 65$, 81, and 97, respectively.

3. Results and discussion

3.1. Selection criteria for electrospray nozzle position

The rate at which the HPLC pumps water through the fraction collector loop into the electrospray mass spectrometer, and the distance between the nozzle and the heated capillary, can be adjusted to optimize signal. The faster a sample is injected into the MS, the higher the flux of ions will be at the electrospray needle, and hence the larger the resulting signal. The maximum injection rate for stable signals was 500 μl min^{-1}. At faster flow rates, the signal was not stable over long periods of time due to increased water vapor in the ionization region, which shorted the electrospray needle to ground. Optimal mass-to-charge signal was obtained when the nozzle was fully retracted to maximize the distance between the electrospray and the heated capillary tube. This position has several advantages. The chance of arcing between the electrospray needle and the heated capillary due to the high voltage (8 kV) on the needle is reduced by maximizing the distance between the two. The increased distance also provides more time for the droplets to break apart before entering the heated capillary. This was further improved by having the sheath gas set at 80 (arbitrary units), above the normal range for this sample flow rate. Despite injecting a matrix of 100% water at 500 μl min^{-1}, when the nozzle was fully retracted and the sheath gas was set appropriately, the IC/ESI-MS system was stable over periods of at least 5 h without shutting down the system to dry the ionization region.

3.2. The ion chromatograph–mass spectrometer interface

Backpressure problems prevent the IC effluent from being connected to the ESI–MS inlet directly. With 4 mm columns and a flow rate of 1.5 ml min^{-1}, the resulting backpressure through the silicon capillary tubing on the ESI-MS is calculated to be 3100 kPa. The maximum allowable backpressure limited by the membranes in the suppressor is 690 kPa. Approximately 280 kPa of backpressure is optimal, so that dissolved gasses do not come out of solution and form bubbles in the conductivity cell. On an IC system used without the effluent being directed into a secondary detector, this backpressure is applied via a coil placed between the conductivity cell and the waste line. In this study the

backpressure coil was removed from the waste line to interface the IC with the ESI-MS.

The backpressure of the system could be reduced to ≤690 kPa by reducing the eluent flow rate to ~100 μl min⁻¹, which can be achieved using a microbore IC system equipped with a 2 mm column. However, to maintain reasonable retention times and minimize peak broadening due to longitudinal diffusion [23], eluent concentrations would need to be increased above the 100 mM concentrations achievable using electrolytic eluent generation. Moreover, increasing the hydroxide concentration would also require that the suppressor current be increased, resulting in a shorter suppressor lifetime, and should any of the tubing become obstructed, the resulting backpressure could damage the suppressor. It should be noted that other ESI-MS systems, such as the ThermoFinnigan MSQ Plus, offer a decreased amount of backpressure for a given flow rate, as compared to the LCQ-Deca employed in this study. This system allows effluent flow rates as high as 1 ml min⁻¹ to be directly connected to the mass spectrometer without exceeding the allowable backpressure on the suppressor.

Rather than connect the IC directly to the ESI-MS, a six-port injector depicted in Fig. 1 equipped with a 20 μl loop was used to collect fractions and then inject full-loop fractions into the mass spectrometer. This loop was chosen because with an I.D. of 0.05 cm, the loop will not contribute significantly to the backpressure on the system. When the injector is in the load position, the IC effluent flows through the loop and then out to waste. During this time, the water from the HPLC pump is plumbed directly into the mass spectrometer. When the valve is switched to the inject position, the HPLC pump pushes the IC fraction out of the loop and into the MS, while the IC effluent stream is directed to waste.

To achieve optimal limits of detection for phosphorus oxyanions, the optimal time for the valve to remain in the load and inject positions needed to be determined. Switching every second and every 2 s was tested, and it was found that switching positions every second produced the best signal. There were two contributing factors that made this arrangement optimal. The first was that by taking fractions at a faster rate, there was a greater probability that the fractions sampled would contain the peak maximum. The other contributing factor was that shorter fraction collection times and shorter analysis times produced a more stable signal because there were fewer times when multiple spectra would contain no ions of interest. The time in each valve position could not be lowered to less than 1 s because of the time it would take to fill the 20 μl loop.

3.3. Ion chromatography separation coupled with ESI mass spectrometry specificity

Previous work performed in our laboratory used suppressed ion chromatography coupled with a conductivity detector to identify phosphorus oxyanions in a synthetic geothermal water matrix [14]. The 3σ limits of detection (LODs) were 0.83, 0.39, and 0.35 μM for hypophosphite, phosphite, and phosphate, respectively. One of the challenges of detecting phosphorus oxyanions in this matrix is that the two reduced forms,

hypophosphite and phosphite, have very similar retention times to fluoride and hydrogen carbonate, respectively, which have relatively large synthetic geothermal water concentrations of 0.43 and 8.1 mM, respectively. A typical strategy to improve the LOD for a given compound is to increase the sample size by increasing the injection loop volume. Unfortunately, with the suppressed conductivity system, when the injection loop size was increased, the peaks corresponding to fluoride and hydrogen carbonate became so large that they completely engulfed the neighboring reduced phosphorus oxyanion peaks. Therefore, optimal limits of detection were achieved by diluting the sample to 25% of its original concentration, and injecting the sample with a 15 μl injection loop. Increasing the loop size or sample concentration negatively impacted the ability to resolve hypophosphite from fluoride and phosphite from hydrogen carbonate.

For the current study, the McDowell et al. gradient was modified slightly, so that during the times when the fluoride/hypophosphite and phosphite/hydrogen carbonate pairs were eluting from the column, the gradient was held at a constant concentration. This technique produces a flatter baseline while the reduced phosphorus oxyanion species were eluting, which slightly improves the limits of detection. Fig. 2 shows the ion chromatograph obtained using the conductivity detector for a 1:4 dilution of synthetic geothermal water spiked with hypophosphite, phosphite and phosphate at concentrations of 10 μM each, injected using a 15 μl injection loop, using the modified gradient program. Even with the improved gradient, the sample size cannot be increased significantly due to the poor resolution between fluoride and hypophosphite (peaks 1 and 2) and phosphite and hydrogen carbonate (peaks 6 and 7).

It was found that introducing samples containing salts fouled the mass spectrometer. A periodic drop in instrument sensitivity, which could be restored by cleaning the API Stack and the heated
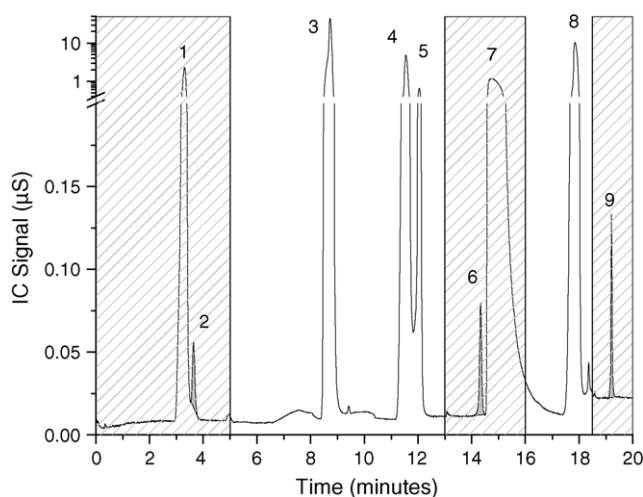

Fig. 2. Conductivity detector data for a 1:4 dilution of synthetic geothermal water spiked with hypophosphite, phosphite and phosphate at concentrations of 10 μM each injected using a 15 μl injection loop. The peak assignments are: (1) flouride; (2) hypophosphite; (3) chloride; (4) bromide; (5) nitrate; (6) phosphite; (7) hydrogen carbonate; (8) sulphate; and (9) phosphate. The hatched areas show when fractions were directed into the ESI-MS.

capillary tube, was attributed to the buildup of salts. Therefore although mass spectrometer data was collected continuously throughout the 20 min run, sample was only introduced into the mass spectrometer during retention windows when phosphorus oxyanions were expected to elute. The hatched areas in Fig. 2 shows the times when sample is analyzed by the mass spectrometer (0–5 min, 13–18 min and 18.5–20 min). By diverting the IC effluent at all other retention times, chloride, bromide, nitrate and sulfate are not introduced into the mass spectrometer, extending the analysis time of the instrument between cleanings. Data collected outside of these windows is the background observed as the HPLC effluent flows into the mass spectrometer.

When using only conductivity detection, it is necessary to have good chromatographic separation because this detector is not specific to a particular ion; only the presence of ions is indicated, with no other information as to their identity. When using mass spectrometry as a detector, it is less important to have complete chromatographic separation as long as the ion of interest has a different mass than other ions, and the presence of these other ions does not cause a significant decrease in the analyte ion signal.

Fig. 3 shows the ion chromatograph for full strength synthetic geothermal water spiked with $10\,\mu M$ each of hypophosphite, phosphite and phosphate injected using a $15\,\mu l$ injection loop, using sequential conductivity and ESI-MS detectors. For the MS data, full scale spectra were collected from $m/z = 50$ to 100, and chromatograms for hypophosphite ($m/z = 65$) phosphite ($m/z = 81$) and phosphate ($m/z = 97$) were plotted. The conductivity data show that when the sample is injected at full strength, hypophosphite and phosphite are no longer resolved from nearby fluoride and hydrogen carbonate peaks, but the mass spectral data show that even in the presence of other ions, there are distinct, narrow peaks for the reduced phosphorus oxyanions. The signal assigned to phosphate has a very noisy background, which is due to a peak in the background that appears at $m/z = 97$, and therefore MS can be used to confirm the identity of phosphate, but under these experimental conditions, IC with conductivity detection is a better technique for monitoring this species.
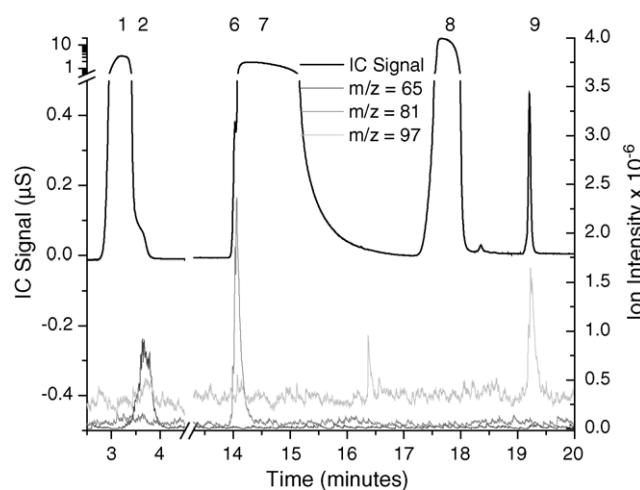

Fig. 3. Conductivity and ESI-MS data for full strength synthetic geothermal water spiked with hypophosphite, phosphite and phosphate at concentrations of $10\,\mu M$ each injected using a $15\,\mu l$ injection loop. Conductivity data (black line) is scaled on the left axis, and ESI-MS data (grey lines) are scaled on the right axis. Peak labels are defined in Fig. 2.

3.4. Quality of chromatography data with increased sample volume

Increasing the sample loop size on the IC will increase the volume of sample that travels to the mass spectrometer, which should yield better limits of detection. Fig. 4 shows ESI-MS data for (a) hypophosphite, (b) phosphite, and (c) phosphate for ion chromatograph injection loop sizes of 8, 15, 20, 30, and $50\,\mu l$. As the loop size increases, the hypophosphite peak gets taller and wider, and the leading edge shifts to earlier retention times. The shape of this peak is attributed to the fact that at larger loop sizes, the column is becoming overloaded and that immediately after injection, more strongly bound species fill up all of the binding sites. Some fraction of the weakly bound ions such as fluoride and hypophosphite will move further down the column before they can find available sites to bind, and these ions will have an earlier retention time. Other hypophosphite ions are able to bind initially, and so this group of ions will have the later
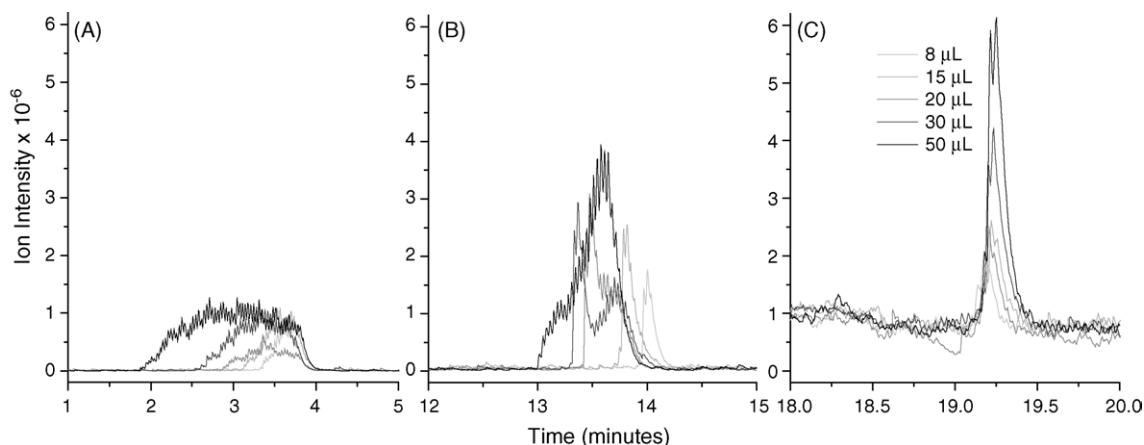

Fig. 4. Electrospray mass spectrometer data for full strength synthetic geothermal water spiked with hypophosphite, phosphite and phosphate at concentrations of $10\,\mu M$ each injected using loop sizes 8–$50\,\mu l$. Panels A–C present $m/z = 65$, 81, and 97 data, respectively.

retention time characteristic of smaller loop sizes. This leads to a broad hypophosphite peak that is spread over more than 2 min for injection loop sizes over 30 μl.

The peak shape and retention time of phosphite (Fig. 4B) are affected differently than hypophosphite as the loop size increases. Phosphite has a very similar retention time to hydrogen carbonate, which at a concentration of 8.1 mM is the most abundant ion in this matrix. Unlike hypophosphite, which is mainly competing for binding sites at the beginning of the column, the similar affinity of phosphite and hydrogen carbonate towards the stationary phase cause them to compete the entire length of the column. Hydrogen carbonate is slightly more strongly bound, resulting in a retention time that is slightly later than phosphite. When the injection loop size increases, the amount of hydrogen carbonate increases filling most available binding sites. Some hydrogen carbonate and the more weakly bound phosphite are pushed ahead in the column. The result is a hydrogen carbonate peak that gets wider as loop size increases, with a leading edge that is pushed to earlier retention times. At larger loop sizes, the phosphite peak is no longer baseline resolved from hydrogen carbonate, and elutes at the same time as the leading edge of the hydrogen carbonate peak. Therefore the entire phosphite peak is pushed to earlier retention times. For sample loops larger than 15 μl, the phosphite signal develops a second peak at a retention time ∼30 s behind the first phosphite peak. For the 50 μl sample loop, this second peak is the predominant phosphite peak. After the column was cleaned using a 80% tetrahydrofuran, 20% 1 M HCl solution [24], this second peak disappeared, and for a 50 μl sample loop, only a single peak with a retention time of 13.3 min was present (see Fig. 5B). Therefore, this second peak at a later retention time has been attributed to contaminants on the column creating a second set of binding sites that have a slightly stronger affinity for phosphite, and will only participate in chromatography at higher column loading.

As the sample loop size increases, the shape and retention time (Fig. 4C) of phosphate is not significantly affected. This is because the phosphate peak is well resolved from neighboring peaks, and therefore is not undergoing increasing competition for sites with other species as the sample size is increased.

A sample loop size of 50 μl was selected from the 8 to 50 μl injection loop size range, because the peak heights for all three phosphorus oxyanion species were largest for this loop size, which would yield the best limit of detection. Larger sample volumes were not employed with these samples because the broad shape of these peaks provided evidence of column overload.

3.5. Quality of chromatography data with 50 μl injection loop and simplified matrix

The synthetic geothermal matrix was simplified by removing chloride, bromide, and hydrogen carbonate ions from the matrix by filtering samples with OnGuard II silver and sulfonic acid cartridges prior to analysis. It was found that filtering synthetic geothermal water in this manner removed 99.96% of the chloride, 100% of the bromide, and the hydrogen carbonate peak was reduced to 47% of its original value. It is impossible to remove all of the hydrogen carbonate, due to equilibrium with carbon dioxide in the air above the samples. Peak areas measured with suppressed conductivity were used to determine the percent recovery and reproducibility of the three phosphorous oxyanions when synthetic geothermal water solutions containing 1.0–8.0 μM of each oxyanion treated with both the silver and sulfonic acid cartridges. Seven samples injected with a 3.8 μl loop were analyzed by this method. For each sample, only 0.9 ± 0.3 μM of phosphate remain in solution after treatment with OnGuard II cartridges in agreement with solubility data that predicts silver phosphate will precipitate out of solution [19]. 52 ± 7% of the phosphite was removed by the OnGuard II cartridges. The overlap between hypophosphite and fluoride were so severe, that it was not possible to quantify the percent recovery of hypophosphite. It was found that the amount removed for all three phosphorus oxyanions was dependent upon the composition of the other ions in solution. Therefore, when calibrating using standards, it is necessary to utilize standards in a similar matrix as the samples to be analyzed, and to pre-treat standards and samples in the same manner.

Even though some hypophosphite and phosphite were removed, the limits of detection were greatly improved by pre-
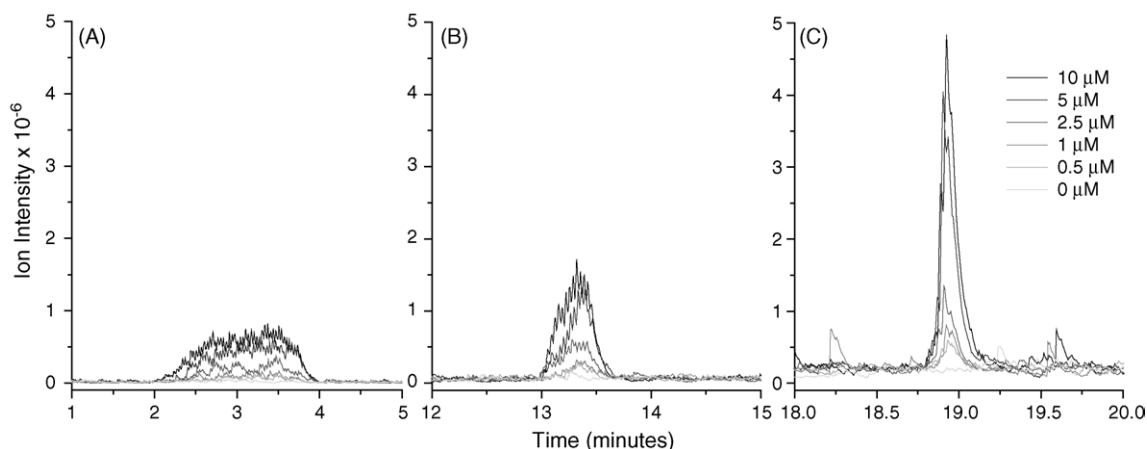

Fig. 5. Electrospray mass spectrometer data for full strength synthetic geothermal water spiked with hypophosphite, phosphite and phosphate at concentrations of 0.0–10 μM each injected using a 50 μl injection loop.
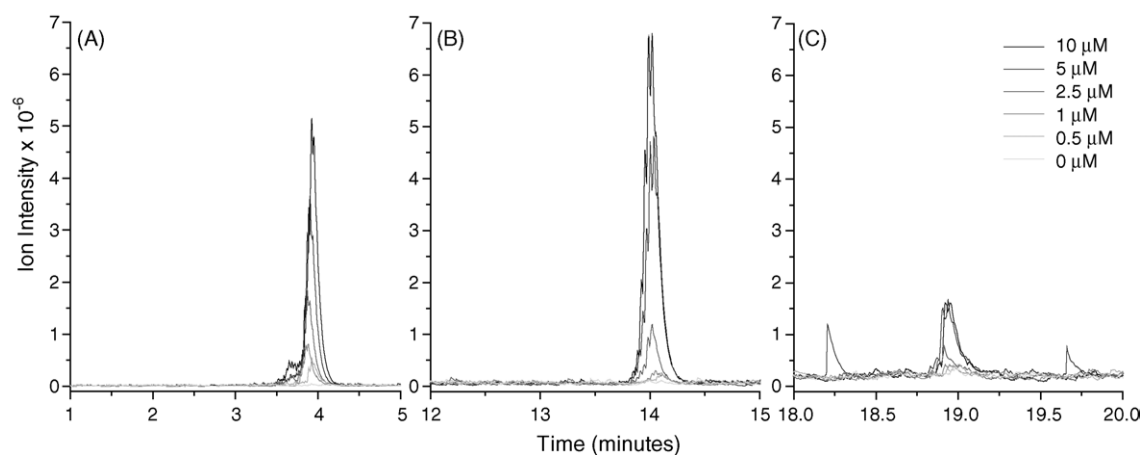
Fig. 6. Electrospray mass spectrometer data for full strength synthetic geothermal water spiked with hypophosphite, phosphite and phosphate at concentrations ranging from 0 to 10 μM and pre-treated with both silver and sulfonic acid cartridges prior to injection using a 50 μl injection loop.

treating the samples. Fig. 5A shows the mass spectral data for hypophosphite with concentrations ranging from 0 to 10 μM in synthetic geothermal water, and Fig. 6A shows the same standards after pre-treatment, analyzed in the same manner as the untreated samples. For the untreated samples, the hypophosphite peak begins at an early retention time (∼2 min) and is almost 2 min in width. For the pre-treated samples, the hypophosphite peak is much narrower (full-width-half-maximum of 0.11 min) and has a retention time of ∼4.0 min, which is characteristic of hypophosphite that is in a matrix of pure water. At first glance, it is somewhat surprising that pre-treatment affects the shape of the hypophosphite peak so drastically, because it would be assumed that hypophosphite would be influenced most by the presence of fluoride, given that fluoride has a similar retention time to hypophosphite; however, the fluoride concentration is not affected by pre-treatment because unlike other halogen salts, AgF is soluble in water [19]. The peak shape of hypophosphite is affected by the total number of ions in the column, indicating that the broadening of the hypophosphite peak occurs at the beginning of the separation, when all of the ions are initially competing for the same sites. Therefore, eliminating some of the other ions leads to a narrower peak that elutes at a time representative of when hypophosphite is injected without the presence of other ions. When the hypophosphite peak area is compared for pre-treated and untreated samples, it is found that the area decreases by 24% when the samples are pre-treated (Table 1, Figs. 5A and 6A). Even though pre-treating decreases the hypophosphite, the limit of detection decreases from 0.35 for

an untreated sample to 0.047 μM for a pre-treated sample, due to the increase in height as peak width is substantially decreased. Tables 1 and 2 compare the quality of the calibration data of samples before and after pre-treatment with silver and sulfonic acid cartridges. Tables 1 and 2 present peak area and peak height calibrations, respectively.

For untreated samples, analyzed with a 50 μl loop, the phosphite was not resolved from hydrogen carbonate, and eluted at the same time as the leading edge of the very broad (2 min) hydrogen carbonate peak. After pre-treatment, the hydrogen carbonate is reduced drastically and the two peaks are baseline resolved. As a result, the retention time of phosphite in pre-treated samples is at the same retention time as that observed when phosphite is diluted in 18.2 MΩ cm water. Because the phosphite ions were no longer competing with hydrogen carbonate ions for binding sites, the peak was slightly narrower. When the areas were compared (Table 1, Figs. 5B and 6B), it was found that the area had doubled for the pre-treated samples, indicating that when phosphite was co-eluting with hydrogen carbonate, the presence of the hydrogen carbonate ions caused a decrease in the instrument sensitivity towards phosphite ions.

In this matrix, phosphate does not have any species with a similar retention time that will compete for binding sites. A comparison of Figs. 5C and 6C show that the retention time of the phosphate peak does not shift when the sample is pre-treated prior to the analysis. A comparison of the peak areas and heights (Tables 1 and 2) show that pre-treatment removes 68% of the phosphate. Therefore, pretreatment does not improve the signal-

Table 1

Peak area calibration parameters for phosphorus oxyanions, 50 μl injection loop

	Hypophosphite		Phosphite		Phosphate	
	Untreated	Pre-treated	Untreated	Pre-treated	Untreated	Pre-treated
Range (μM)	0.0–10.0	0.0–10.0	0.0–10.0	0.0–10.0	0.0–10.0	0.0–10.0
Linear regression coefficient, R^2	0.96	0.97	0.97	0.94	0.92	0.79
Number of data points	6	6	6	6	6	6
Slope ($\times 10^{-3}$) (ion intensity, min μM^{-1})	89 ± 9	68 ± 6	51 ± 5	102 ± 13	46 ± 7	15 ± 4
Intercept ($\times 10^{-3}$) (ion intensity, min)	48 ± 46	37 ± 28	25 ± 22	−27 ± 59	20 ± 31	17 ± 18
Area ratio (untreated:pre-treated)	1: 0.76		1: 2.0		1: 0.32	

Table 2
Peak height calibration parameters and detection limits for phosphorus oxyanions, 50 μl injection loop

	Hypophosphite		Phosphite		Phosphate	
	Untreated	Pre-treated	Untreated	Pre-treated	Untreated	Pre-treated
Range (μM)	0.0–10.0	0.0–10.0	0.0–10.0	0.0–10.0	0.0–10.0	0.0–10.0
Linear regression coefficient, R^2	0.96	0.97	0.97	0.94	0.92	0.79
Number of data points	6	6	6	6	6	6
Slope ($\times 10^{-4}$) (ion intensity, min μM^{-1})	8.1 ± 1.1	52 ± 5	17 ± 2	73 ± 9	49 ± 8	15 ± 4
Intercept ($\times 10^{-4}$) (ion intensity, min)	8.4 ± 5.6	37 ± 26	19 ± 10	-7 ± 41	42 ± 37	37 ± 18
Detection limit, DL (μM)	0.35	0.047	0.48	0.087	0.56	1.21
Height ratio (untreated:pre-treated)	1: 6.4		1: 4.3		1: 0.31	

DL, the detection limit (μM) is three times the standard deviation of the noise for 18.2 MΩ cm water injections.

to-noise of phosphate, with a LOD of 1.21 μM for a pretreated sample and 0.56 μM for an untreated sample, both analyzed with a 50 μl loop using ESI-MS as a detector.

3.6. Larger sample volume to increase phosphite sensitivity

Even though both hypophosphite and phosphite are not thermodynamically stable in the natural environment [7], the ability to store solutions of sodium salts of these ions [14], indicates that these species, if produced in nature, could be stable over a period of time. By examining an equilibrium pe/pH diagram, it is expected that phosphite is a more likely candidate to be found in natural reducing environments such as a geothermal hot spring [7]. Therefore, a method was developed to specifically concentrate on detection of phosphite. The silver cartridge has been shown to decrease the concentrations of phosphite by 48%, and therefore this cartridge was not employed so that the phosphite concentration could be maximized. Pre-treatment with the sulfonic acid cartridge to remove hydrogen carbonate was still performed, because co-eluting hydrogen carbonate ions would result in a loss of phosphite ion signal and because competition between the two ions would result in a broadened peak.

For the detection of phosphite in pre-treated samples, the gradient program for the IC was changed to 3.0–10.5 mM from 0 to 7.5 min; 10.5 mM between 7.5 and 11.5 min; 10.5–41 mM from 11.5 to 13 min; and 41 mM between 13 and 15 min, and the total run time was 15 min. When sample handling is taken into account, ~3.5 samples can be analyzed in an hour, rather than ~2.5 using the old method, which is an advantage when a large number of samples need to be analyzed. By lowering the middle plateau in the gradient to 10.5 mM, the phosphite and hydrogen carbonate spend more time on the column, and the time separating these peak increases to over 1.1 min, as compared to 0.75 min in the original method. By having the peaks more widely separated, it is now possible to increase the loop size to larger volumes before these two peaks are no longer baseline resolved, which would interfere with the analysis of phosphite (Fig. 7).

For a 50 μl loop, phosphite elutes at 9.95 min and hydrogen carbonate elutes at 11.1 min. As the loop size is increased, the sulfate peak gets wider, pushing both phosphite and carbonate to earlier retention times. For an 800 μl loop, phosphite and hydrogen carbonate are only separated by 0.3 min, eluting at 9.1 and 9.4 min, respectively. The conductivity detection and MS

data for 0.1 μM phosphorus oxyanions in synthetic geothermal water show that 800 μl is the largest sample loop size that would still provide baseline separation for phosphite and hydrogen carbonate (Fig. 7). The ESI-MS data clearly show the presence of hypophosphite, phosphite and phosphate peaks, with estimated 3σ limits of detection of 0.011, 0.0020 and 0.029 μM, respectively.

With an 800 μl loop and a flow rate of 1.5 ml min^{-1}, it will take 32 s for the sample to be loaded onto the IC, and a concern was that the use of such a large loop would lead to broadening of the peaks of interest. The IC data clearly shows that the phosphite peak is ~5 s wide (FWHM) and the phosphate peak is ~3 s in width (FWHM), which is significantly shorter than the injection time. During the time when the sample is injected onto the column, the eluent hydroxide ion concentration is fairly low (<3.1 mM), and so phosphite and phosphate ions spend the majority of their time bound to the column, and therefore do not move very far down the column. As the sample is loaded onto the column, the ions will accumulate at the beginning of the column, and will only move a significant distance after the hydroxide ion concentration increases later in the gradient program.
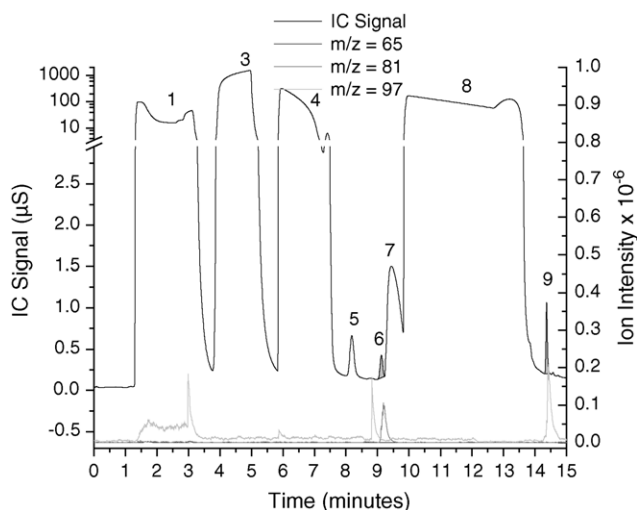

Fig. 7. Conductivity and ESI-MS data for full strength synthetic geothermal water spiked with hypophosphite, phosphite and phosphate at concentrations of 0.10 μM each, and pre-treated with a sulfonic acid cartridge prior to injection using an 800 μl injection loop. Conductivity data (black line) is scaled on the left axis, and ESI-MS data (grey lines) is scaled on the right axis.

4. Conclusions

This study successfully employed a range of injection loop sizes and sample pre-treatment with silver and sulfonic acid cartridges to produce one of the most specific and sensitive phosphorus oxyanion detection techniques available. The technique employs two commercially available instruments, interfaced with a novel pulsed-injection valve. Using ESI-MS as a detector for IC, a 50 µl injection loop, and pre-treatment with silver and sulfonic acid cartridges, the limits of detection for hypophosphite and phosphite were 0.047 and 0.087 µM, respectively. Larger sample volumes can be introduced to the column using larger injection loops to increase sensitivity. The effect of larger loop size was tested for loops up to 800 µl for synthetic geothermal water pre-treated to reduce hydrogen carbonate concentrations. By increasing the injection loop size to 800 µl, and eliminating the silver cartridge from the pre-treatment step of the sample analysis, the limits of detection for hypophosphite and phosphite were decreased to 0.011 and 0.0020 µM, respectively. This is an improvement over IC with suppressed conductivity detection alone, which has limits of detection of 0.83 and 0.39 µM for hypophosphite and phosphite, respectively [14].

Phosphate is significantly reduced by pre-treatment with the silver OnGuard II cartridge, and there the best limits of detection for phosphate analysis were achieved when this cartridge was not employed. For a 50 µl loop, the 3σ limits of detection (0.56 µM) for an untreated sample is not as good as the 0.39 µM limit of detection determined using conductivity detection reported by McDowell et al. [14] in previous work, but the mass spectrometer provides additional specificity, which helps to confirm the presence of the phosphate ion. The 3σ limit of detection was further reduced to 0.029 µM by employing an 800 µl loop and pre-treating samples with a sulfonic acid OnGuard II cartridge.

A variety of IC-MS methods to detect reduced phosphorus oxyanions have been discussed. These methods can be employed to determine if these compounds are present in natural watersheds, which would encourage scientists to reevaluate the role of phosphorus oxyanions in biological systems.

Acknowledgements

References

[1] W.W. Metcalf, R.S. Wolfe, J. Bacteriol. 180 (1998) 5547.
[2] I. Dévai, L. Felföldy, I. Wittner, S. Plósz, Nature 333 (1988) 343.
[3] B.V. Rutishauser, R. Bachofen, Anaerobe 5 (1999) 525.
[4] G. Gassmann, F. Schorn, Naturwissenschaften 80 (1993) 78.
[5] L. Parmeggiani (Ed.), Encyclopedia of Occupational Health and Safety, Industrial Labour Office, Geneva, Switzerland, 1983, p. 1681.
[6] A.E. McDonald, B.R. Grant, W.C. Plaxton, J. Plant Nutr. 24 (2001) 1505.
[7] G. Hanrahan, T.M. Salmassi, C.S. Khachikian, K.L. Foster, Talanta 66 (2005) 435.
[8] K. Robards, I.D. McKelvie, R.L. Benson, P.J. Worsfold, N.J. Blundell, H. Casey, Anal. Chim. Acta 287 (1994) 147.
[9] S.-J. Jiang, R.S. Houk, Spectrochim. Acta, Part B 43 (1988) 405.
[10] M.C. Mehra, C. Pelletier, Anal. Sci. 6 (1990) 431.
[11] B. Divjak, M. Novič, W. Goessler, J. Chromatogr. A 862 (1999) 39.
[12] G.H.P. Roos, C. Loane, B. Dell, G.E.S.J. Hardy, Commun. Soil Sci. Plant Anal. 30 (1999) 2323.
[13] S.C. Morton, D. Glindemann, M.A. Edwards, Environ. Sci. Technol. 37 (2003) 1169.
[14] M.M. McDowell, M.M. Ivey, M.E. Lee, V.V.V.D. Firpo, T.M. Salmassi, C.S. Khachikian, K.L. Foster, J. Chromatogr. A 1039 (2004) 105.
[15] V. Ruiz-Calero, M.T. Galceran, Talanta 66 (2005) 376.
[16] S.C. Morton, D. Glindemann, X. Wang, X. Niu, M. Edwards, Environ. Sci. Technol. 39 (2005) 4369.
[17] J.A.G. Neto, H.A. Ito, K.G. Fernandes, M. de Moraes, A.A. Cardoso, Lab. Rob. Auto. 12 (2000) 286.
[18] R.H. Smillie, B. Grant, R.L. Cribbes, J. Chromatogr. 455 (1988) 253.
[19] D.R. Lide (Ed.), CRC Handbook of Chemistry and Physics, CRC Press, Boca Raton, 1995, p. 4.84.
[20] J.A. Wilkie, Civil Engineering, University of California, Los Angeles, Los Angeles, 1997, p. 81.
[21] Dionex, Product Manual OnGuard II Cartridges, Dionex Corporation, Sunnyvale, 2003, p. 9.
[22] J. Weiss, Handbook of Ion Chromatography, Wiley-VCH Verlag GmbH & Co. KGaA, Weinheim, Verlag, Germany, 2004, p. 835.
[23] H.A. Strobel, W.R. Heineman, Chemical Instrumentation: A Systematic Approach, John Wiley & Sons, New York, 1989, p. 888.
[24] Dionex, IonPac AG17 Manual. Dionex Corporation, Sunnyvale, 2002, p. 27.